

Estimates for the Luminosity Function of Galaxies and its Evolution

Volker Springel and Simon D. M. White

Max-Planck-Institut für Astrophysik, Karl-Schwarzschild-Straße 1, 85740 Garching bei München, Germany

4 August 2021

ABSTRACT

A new method is presented to obtain a non-parametric maximum likelihood estimate of the luminosity function and the selection function of a flux limited redshift survey. The method parameterizes the selection function as a series of step-wise power laws and allows possible evolution of the luminosity function. We also propose a new technique to estimate the rate of evolution of the luminosity function. This is based on a minimization of the observed large-scale power with respect to the evolutionary model. We use an ensemble of mock surveys extracted from a N-body simulation to verify the power of this method.

We apply our estimators to the 1.2-Jy survey of *IRAS* galaxies. We find a far-infrared luminosity function in good agreement with previously published results and evidence for rather strong evolution. If the comoving number density of *IRAS* galaxies is assumed to scale $\propto (1+z)^P$, we estimate $P = 4.3 \pm 1.4 \pm 1$.

Key words: methods: statistical – galaxies: evolution – infrared: galaxies.

1 INTRODUCTION

Flux limited redshift surveys are a major tool for studying the large-scale structure of the Universe. However, such catalogues show a strong decline of the mean number density of galaxies as a function of distance, simply because at larger distances more and more galaxies fall below the apparent flux limit. Most of the statistics that are used to analyse these surveys require an accurate knowledge of this dependence, which is described in terms of the selection function (SF). Hence the accuracy of the adopted SF can limit the reliability of such large-scale structure studies.

Closely related to the SF is the luminosity function (LF), which describes the distribution in luminosity of the galaxy population sampled by the particular redshift survey. This quantity is of more fundamental importance, since it should be reproduced by any viable theory of galaxy formation and evolution.

Here we revisit the problem of determining the LF and SF, given only the data of a flux limited redshift survey. Current standard methods for this task include Schmidt’s (1968) V/V_{\max} estimator, and the maximum likelihood techniques first introduced by Turner (1979) and Sandage, Tamman & Yahil (1979). The maximum likelihood methods are generally superior to the older techniques because they allow the construction of estimators which are not systematically biased by density inhomogeneities. For this reason we will focus on them in the following.

Two basic procedures have been used to find maximum

likelihood estimates of the LF. In the so-called parametric maximum likelihood estimate (Sandage, Tamman & Yahil 1979; Yahil et al. 1991) an analytic form for the LF (or SF) is assumed that depends on a few (typically two to four) parameters. These are then determined by maximizing the likelihood of the observed data set.

However, because the maximum likelihood technique offers no built-in measure of goodness-of-fit, almost any functional form can be made to ‘fit’, although the function may provide only a poor description of the data. The parametric technique therefore requires an *a priori* knowledge of a suitable fitting form.

If this information is not available one can allow a very flexible shape of the LF by describing it by many parameters in a reasonable way. This so-called step-wise non-parametric maximum likelihood method (Nicoll & Segal 1983; Efstathiou, Ellis & Peterson 1988) has been used both to find luminosity functions (Efstathiou, Ellis & Peterson 1988; Loveday et al. 1992; Lin et al. 1996) and to estimate the run of radial density with distance (Saunders et al. 1990; Loveday et al. 1992). So far these applications only employed simple step functions to model the desired function.

In this paper we propose a non-parametric maximum likelihood estimator that uses a new parameterization in terms of piece-wise power laws. This method provides accurate information on the shapes of the SF and the LF and has a number of computational advantages. For example, it does not require iterative solutions and it provides error-

arXiv:astro-ph/9704126v1 14 Apr 1997

estimates easily. The method is particularly useful for justifying specific analytic fitting forms for the SF and LF.

We also discuss ways to estimate evolution of the LF. Such evolution appears quite strong in the far-infrared. A V/V_{\max} test may be used to estimate the evolutionary rate (Avni & Bahcall 1980), but the result can be strongly affected by density inhomogeneities. Saunders et al. (1990) proposed an alternative maximum likelihood estimator for density evolution. Unfortunately, their technique is troubled by the same problem; it explicitly assumes a locally uniform distribution of galaxies. In order to reduce the influence of density inhomogeneities (which are clearly present) we propose to combine the SF determination with a counts-in-cells analysis on large scales. The evolutionary rate is then estimated by minimizing the variance of the large scale density field. We demonstrate the robustness of this method using an ensemble of flux limited mock catalogues constructed by observing an N-body model universe.

Our paper is organized as follows. Sections 2 and 3 present in detail our non-parametric estimators for the SF and the LF. The estimation of evolution is discussed in section 4. Finally, we apply these methods in section 5 to the 1.2-Jy survey of *IRAS* galaxies. In particular, we give results for the far-infrared LF, its evolution and the SF of the 1.2-Jy survey.

2 A NON-PARAMETRIC ESTIMATOR FOR THE SELECTION FUNCTION

2.1 Definitions

Let the field $n_z(\mathbf{r}, L) dL$ describe the comoving number density of galaxies at epoch z , in the luminosity interval $[L, L + dL]$ and at comoving spatial position \mathbf{r} . Assuming that the luminosity distribution is independent of clustering the number density field may be written as

$$n_z(\mathbf{r}, L) = \frac{n_z(\mathbf{r})}{\bar{n}_z} \Phi_z(L), \quad (1)$$

where $\Phi_z(L)$ describes the LF. Here $n_z(\mathbf{r}) = \int_{L_0}^{\infty} n_z(\mathbf{r}, L) dL$ is the local number density and $\bar{n}_z = \langle n_z(\mathbf{r}) \rangle$ signifies the mean number density, averaged over many realizations of the Universe. The LF is normalized as $\int_{L_0}^{\infty} \Phi_z(L) dL = \bar{n}_z$ and the dependence on z takes care of a possible time evolution, if present. The luminosity cut L_0 may be used to handle a possible formal divergence of the integral over $\Phi_z(L)$ at the lower end.

We define the selection function $S(z)$ as the mean comoving number density of galaxies that one expects to see in a flux limited survey at redshift z . Then $S(z)$ is given by

$$S(z) = \int_{L_{\min}(z)}^{\infty} \Phi_z(L) dL, \quad (2)$$

where $L_{\min}(z)$ denotes the minimum luminosity a source at redshift z may have without falling below the flux limit of the catalogue. In this work we neglect the peculiar velocities of galaxies and take all redshifts to be cosmological, i.e. we adopt a simple redshift-distance relation $z = z(|\mathbf{r}|)$.

2.2 The likelihood expression

We now imagine that the catalogue is drawn from an underlying parent distribution given by $n_z(\mathbf{r}, L)$ for $L \geq L_{\min}(z)$ and by 0 for $L < L_{\min}(z)$, where $z = z(\mathbf{r})$. Then the conditional probability $p(L_i|z_i) dL$ that a source observed at redshift z_i falls into the luminosity range $[L_i, L_i + dL]$ takes the form

$$p(L_i|z_i) dL = \frac{n_{z_i}(\mathbf{r}_i, L_i) dL}{\int_{L_{\min}(z_i)}^{\infty} n_{z_i}(\mathbf{r}_i, L') dL'}. \quad (3)$$

The denominator simply counts the available number of galaxies at that distance and the numerator gives the number of galaxies in the particular luminosity range. Upon insertion of equations (1) and (2) this becomes

$$p(L_i|z_i) = \frac{\Phi_{z_i}(L_i)}{S(z_i)}. \quad (4)$$

Note that the density fluctuations have dropped out of this expression and so the dependence on \mathbf{r} can be dropped in equation (3). This insensitivity to density inhomogeneities makes the maximum likelihood technique used here superior compared to older methods like the ordinary V/V_{\max} estimator. If one now maximizes the likelihood

$$\mathcal{L} = \prod_i p(L_i|z_i) \quad (5)$$

of the whole data set with respect to $S(z)$ one obtains an estimate of the SF that is not systematically biased by local density fluctuations.

In order to find this maximum in practice we first express $\Phi_{z_i}(L_i)$ in terms of the SF with the help of equation (2). Here a model for the evolution of the LF has to be specified. For brevity we will only treat a case with pure density evolution according to

$$\Phi_z(L) = g(z) \Phi_0(L). \quad (6)$$

However, our method can be easily generalized to include luminosity evolution as well.

We further define a maximal redshift z_i^m for each source such that $L_{\min}(z_i^m) = L_i$. If then the derivative $S'(z)$ of equation (2) is evaluated at z_i^m one obtains

$$S'(z_i^m) = -\frac{g(z_i^m)}{g(z_i)} \Phi_{z_i}(L_i) L'_{\min}(z_i^m) + \frac{g'(z_i^m)}{g(z_i^m)} S(z_i^m), \quad (7)$$

so that the probability of equation (4) can be expressed entirely in terms of $S(z)$ and $g(z)$. Hence one finally has to maximize

$$\begin{aligned} \Lambda = \ln \mathcal{L} &= \sum_i \ln \left(\frac{-S'(z_i^m)}{S(z_i)} + \frac{g'(z_i^m)}{g(z_i^m)} \frac{S(z_i^m)}{S(z_i)} \right) \\ &+ \sum_i \ln \left(\frac{g(z_i)}{g(z_i^m)} \right) - \sum_i \ln L'_{\min}(z_i^m), \end{aligned} \quad (8)$$

where the constant sum of the last term may be dropped.

The above form suggests that one might be able to maximize Λ simultaneously for $g(z)$ and $S(z)$. However, if equation (4) is rewritten for the density evolution model it becomes

$$p(L_i|z_i) = \frac{g(z_i) \Phi_0(L_i)}{\int_{L_{\min}(z_i)}^{\infty} g(z_i) \Phi_0(L) dL} = \frac{\Phi_0(L_i)}{\int_{L_{\min}(z_i)}^{\infty} \Phi_0(L) dL}.$$

So the function $g(z)$ drops out completely and there is no sensitivity to density evolution with this estimator. In fact, this was to be expected since estimates based on the likelihood (4) are independent of the density distribution by construction.

2.3 A non-parametric maximum likelihood estimator

Here we propose a new variant of the non-parametric method that models $S(z)$ as a series of continuously linked power laws. This description seems appropriate since the SF is a smooth curve that covers a wide range of values and its local behaviour can be very well approximated by a power law.

We describe $S(z)$ by n pieces. Let $S_k = S(x_k)$ be the values of $S(z)$ at a series of ascending redshifts x_k where $k \in \{1, 2, \dots, n\}$. Then bin 1 covers $0 < z \leq x_1$, bin 2 covers $x_1 < z \leq x_2$, and so forth. In each piece k , $S(z)$ is taken to be a power law of the form

$$S(z) = S_k \left(\frac{z}{x_k} \right)^{m_k} \quad \text{for } x_{k-1} < z \leq x_k, \quad (9)$$

where m_k is the logarithmic slope of the particular piece. These slopes are precisely the quantities needed to characterize the shape of the SF.

The different pieces have to join continuously, because $S(z)$ is an integral over the LF. Continuity requires the S_k to be related by

$$S_k = S_1 \prod_{j=2}^k \left(\frac{x_j}{x_{j-1}} \right)^{m_j} \quad \text{for } 1 < k \leq n. \quad (10)$$

Let us further define a_i as the number of the bin to which the maximal redshift z_i^m of galaxy i belongs. Similarly, let b_i be the number of the interval that encloses the redshift z_i of galaxy i . Then the likelihood (8) takes the form

$$\begin{aligned} \Lambda = & \sum_i \left[\ln \left(\frac{-m_{a_i}}{z_i^m} + \frac{g'(z_i^m)}{g(z_i^m)} \right) + \sum_{j=b_i+1}^{a_i} m_j \ln \frac{x_j}{x_{j-1}} \right] \\ & + \sum_i m_{a_i} \ln \frac{z_i^m}{x_{a_i}} - \sum_i m_{b_i} \ln \frac{z_i}{x_{b_i}} \\ & + \sum_i \ln \frac{g(z_i)}{g(z_i^m)} - \sum_i \ln L'_{\min}(z_i^m). \end{aligned} \quad (11)$$

The best estimates for the m_k can be found by solving the likelihood equations

$$\frac{\partial \Lambda}{\partial m_k} = \sum_i \frac{\delta_{k,a_i}}{m_k - z_i^m \frac{g'(z_i^m)}{g(z_i^m)}} + T_k = 0, \quad (12)$$

where T_k is defined as

$$\begin{aligned} T_k = & \sum_i \sum_{j=b_i+1}^{a_i} \delta_{j,k} \ln \frac{x_j}{x_{j-1}} + \sum_i \delta_{k,a_i} \ln \frac{z_i^m}{x_{a_i}} \\ & - \sum_i \delta_{k,b_i} \ln \frac{z_i}{x_{b_i}}. \end{aligned} \quad (13)$$

The equations (12) are not fully linear in m_k , but *almost*. Since the redshift bins are narrow, replacing z_i^m by x_{a_i} will give a useful first approximation \tilde{m}_k to the true solution

m_k , which might then quickly be improved by an iteration technique. This starting value can be calculated as

$$\tilde{m}_k = -\frac{n_k}{T_k} + x_k \frac{g'(x_k)}{g(x_k)}, \quad (14)$$

where n_k is the number of galaxies in bin k . Note that in the case of no evolution the solution to equation (12) is simply given by $m_k = -n_k T_k^{-1}$.

The maximum likelihood method also allows an estimate of the statistical uncertainties of the derived parameters (Kendall & Stuart 1979). Asymptotically the distribution of \mathcal{L} is a multivariate Gaussian around the true values of the parameters. If the information matrix I is defined as

$$I_{ij} = -\frac{\partial^2 \Lambda}{\partial m_i \partial m_j}, \quad (15)$$

then the covariance matrix of the parameter estimates is given by $\text{cov}(m_i, m_j) = (I^{-1})_{ij}$ evaluated at the maximum of Λ . This result holds asymptotically for large sample sizes.

Because the T_k don't explicitly depend on any of the m_k the information matrix is simply found to be

$$I_{kk} = \delta_{i,k} \sum_i \frac{\delta_{k,a_i}}{\left(m_k - z_i^m \frac{g'(z_i^m)}{g(z_i^m)} \right)^2}. \quad (16)$$

One can therefore trivially invert this diagonal matrix and find error estimates for the m_k as

$$\text{var}(m_k) = \left[\sum_i \delta_{k,a_i} \left(m_k - z_i^m \frac{g'(z_i^m)}{g(z_i^m)} \right)^{-2} \right]^{-1} \simeq \frac{m_k^2}{n_k}. \quad (17)$$

This is a surprisingly simple result. In particular, one can solve for each of the m_k independent of all the others. The m_k are mutually uncorrelated which shows that it is essentially the local logarithmic slope of the SF that is determined by the maximum likelihood estimator (5).

Once the non-parametric estimate of the shape of the SF is found, it can be used to find and justify an appropriate analytic fitting function for $S(z)$. For this purpose one can directly employ a minimum χ^2 fit of the m_k to the logarithmic slope of some fitting form for $S(z)$. Of course, once an analytic form has been selected in this way, the values of its parameters can also be determined with the parametric maximum likelihood technique by using the fitting form directly in equation (8).

2.4 Normalization

Because the normalization of the SF is lost with the above estimator it has to be found in a second step. For this purpose we write the SF as

$$S(z) = \psi s(z), \quad (18)$$

where $s(z)$ is the shape of the SF as determined above. Then an unbiased estimate $\tilde{\psi}$ of the factor ψ is given by

$$\tilde{\psi} = \frac{\int_V m(\mathbf{r}) w(\mathbf{r}) d\mathbf{r}}{\int_V s(\mathbf{r}') w(\mathbf{r}') d\mathbf{r}'} \quad (19)$$

for an arbitrary weight function $w(\mathbf{r})$. Here $m(\mathbf{r}) = \sum_i \delta(\mathbf{r} - \mathbf{r}_i)$ represents the observed galaxy field and we employ the shorthand notation $s(\mathbf{r}) = s(z(|\mathbf{r}|))$.

Following Davis & Huchra (1982) we choose the weight function $w(\mathbf{r})$ such that the expected variance of $\tilde{\psi}$ is minimized. This is to a good approximation the case for

$$w(\mathbf{r}) = \frac{1}{1 + J_3 \tilde{\psi} s(\mathbf{r})}, \quad (20)$$

where $J_3 = \int_V 4\pi r^2 \xi(r) dr$ is the second moment of the two-point correlation function and V denotes the volume used in the normalization.

Note that the normalization estimate has to be found iteratively since the estimator depends implicitly on $\tilde{\psi}$. One also needs a model for the two-point correlation function in order to estimate J_3 . However, this is uncritical because the dependence on J_3 is usually quite weak. Hence an estimate of J_3 based on a linear theory CDM power spectrum should be entirely sufficient.

The numerical value of $\tilde{\psi}$ itself does not provide a meaningful measure for the local number density of galaxies. In fact, such a measure is not well defined for a purely flux limited catalogue. Instead, the normalization is perhaps best expressed in terms of the expected number density N of galaxies per unit solid angle on the sky, i.e.

$$N = \frac{1}{4\pi} \int S(z) \frac{dV}{dz} dz. \quad (21)$$

3 A NON-PARAMETRIC ESTIMATOR FOR THE LUMINOSITY FUNCTION

Using equation (2) it is possible to recover the underlying luminosity distribution if the SF is known, or vice versa. In particular one can readily derive a non-parametric LF estimate from the SF estimator described in the previous section.

We suppose that the SF has been determined with the estimator described above and that the function $L_{\min}(z)$ and its inverse $z_{\max}(L)$ are known. The piecewise description of the SF directly translates into a piecewise description of the LF if boundaries L_k of luminosity intervals are defined by $L_k \equiv L_{\min}(x_k)$. Upon evaluation of the derivative of equation (2) at $z = z_{\max}(L)$ the present day LF results as

$$\begin{aligned} \Phi_0(L) &= \left(\frac{g'(z_{\max})}{g(z_{\max})} S(z_{\max}) - S'(z_{\max}) \right) \\ &\times \left(g(z_{\max}) L'_{\min}(z_{\max}) \right)^{-1}. \end{aligned} \quad (22)$$

This translates into the piecewise description

$$\begin{aligned} \Phi_0(L) &= \left(\frac{g'(z_{\max})}{g(z_{\max})} - \frac{m_k}{z_{\max}} \right) \left(\frac{z_{\max}}{x_k} \right)^{m_k} \\ &\times \frac{S_k}{g(z_{\max}) L'_{\min}(z_{\max})} \end{aligned} \quad (23)$$

for $L_{k-1} < L < L_k$, which is the desired non-parametric estimate.

The usual way to find a non-parametric maximum likelihood estimate of the LF utilizes a parameterization by a series of step functions (Efstathiou, Ellis & Peterson 1988; Loveday et al. 1992). We see two main advantages of our method as compared to this approach.

First, the shape of the LF over each bin is approximately a power law, so it is able to adapt to the true

shape of the LF in a flexible way. Only very small discontinuities at the boundaries of bins remain and the estimate $\Phi_0(L)$ of equation (23) traces the smooth LF quite well. The conventional estimator on the other hand assumes constant Φ_0 over each bin which leads to large discontinuous jumps in the LF at bin boundaries. Efstathiou et al. (1988) show that the heights Φ_k of these bins are related by $\Phi_k \approx \int_{L_k - \Delta L/2}^{L_k + \Delta L/2} \Phi dN(L) / \int_{L_k - \Delta L/2}^{L_k + \Delta L/2} dN(L)$ to the underlying luminosity distribution. It is therefore more complicated to infer the smooth underlying LF from this non-parametric estimate.

A second nice feature is that the absence of correlations among the m_k simplifies the estimation of errors in the LF. To demonstrate this let us define the values $\Phi_k \equiv \Phi_0(L_k)$ of the LF at the points L_k . In appendix A we compute the covariance matrix

$$V_{kl} = \text{cov}(\ln \Phi_k, \ln \Phi_l) \quad (24)$$

of these quantities. The matrix V_{kl} may then be used to fit an analytic model $\tilde{\Phi}_k$ to the non-parametric LF estimate by minimizing the covariance form

$$\chi^2 = \sum_{l,k} (\ln \Phi_l - \ln \tilde{\Phi}_l) V_{lk}^{-1} (\ln \Phi_k - \ln \tilde{\Phi}_k). \quad (25)$$

Although not of major importance a further practical advantage of the estimator presented here is its relative computational ease. In particular one does not have to resort to lengthy iteration techniques as required by the conventional parameterization with a series of step functions.

4 ESTIMATING EVOLUTION

4.1 The radial density distribution

As was demonstrated above, the estimators based on equation (4) are insensitive to density evolution. If the latter is important (as appears to be the case in the *IRAS* surveys) a different approach is needed to determine its rate.

Instead of $p(L_i|r_i)$ as before we can equally well write down the conditional probability

$$p(r_i|L_i) dr = \frac{4\pi r_i^2 n_{z_i}(r_i, L_i) dr}{\int_0^{r_i^*} n_{z_i}(r, L_i) dV} = \frac{4\pi r_i^2 n_{z_i}(r_i) dr}{\int_0^{r_i^*} n_z(r) dV} \quad (26)$$

to find a galaxy with luminosity L_i in a distance interval of width dr at coordinate $r_i < R_{\max}$. Here the density field has been averaged over direction and the definition $r_i^* \equiv \min(r_i^m, R_{\max})$ allows an upper distance cut-off R_{\max} to be included. We consider the inclusion of the latter to be important because the density field is only known well to a finite depth. At large distances it is dominated by shot noise due to increasingly sparse sampling. In addition the completeness of most surveys is worst in this regime.

Equation (26) shows that the density distribution $n_z(r)$ can be estimated independent of the LF if

$$\Lambda = \sum_i \ln p(r_i|L_i) = \sum_i \ln \frac{n_{z_i}(r_i)}{\int_0^{r_i^*} n_{z(r)}(r) dV} \quad (27)$$

is maximized with respect to $n_z(r)$. Saunders et al. (1990) have used a parameterization of $n_z(r)$ in terms of a series of step functions leading to a non-parametric radial density

estimator. This estimator is quite useful since it can indicate the presence of evolution and it can show the most prominent density features.

4.2 The constant density method

In order to obtain an estimate of the evolutionary rate Saunders et al. (1990) proposed replacing $n_z(r)$ in equation (26) by the expected mean density $\bar{n}_z = \bar{n}_0 g(z)$ at epoch $z = z(r)$. Adopting an evolutionary model, for example

$$g(z) = (1+z)^P, \quad (28)$$

one can then find the rate by maximizing

$$\Lambda = \sum_i \ln \frac{(1+z_i)^P}{\int_{z_{\min}}^{z_i^*} (1+z)^P \frac{dV}{dz} dz} \quad (29)$$

with respect to P . A number of subsequent studies (Fisher et al. 1992; Oliver et al. 1994) also applied this method to *IRAS* galaxies.

Of course, in reality the galaxies are not distributed uniformly. This fact leads to a serious drawback of the above estimator; the resulting estimate of P can be strongly influenced by density inhomogeneities. For example, an overdensity in the foreground mimics negative evolution, whereas an overdensity in the background can bias the evolution low.

Since this effect should be strongest nearby, a lower redshift cut-off z_{\min} , as introduced above, may be used to partly reduce its influence. However, as will be seen in our application to the 1.2-Jy survey the evolutionary estimates can depend quite strongly on the particular redshift interval chosen and it is unclear which choice gives the most reliable answer.

4.3 The minimal variance method

We here want to propose an alternative evolutionary estimator that avoids the unphysical neglect of density fluctuations and that gets rid of the arbitrary choice of redshift interval used in equation (29).

As shown above the data of the redshift survey alone do not allow us to disentangle density evolution and large-scale structure. This is only possible if the fundamental assumption of statistical homogeneity is added. In a pragmatic approach we might then base the determination of evolution on the notion that the correct rate should lead to a universe that looks as close as possible to homogeneous on very large scales. As a quantitative measure for deviations from homogeneity one might, for example, take the variance σ^2 of the density field smoothed on some large scale λ . The determination of the evolution might therefore be formulated in terms of an extremal principle: The evolutionary rate can be estimated by minimizing the observed power on large scales.

To estimate σ^2 we apply a slightly modified version of the method of Saunders et al. (1991). We first compute a smoothed galaxy density field

$$d_i = \sum_j w_{ij} \frac{m_j}{S_j} \quad (30)$$

on a fine mesh. Here m_j denotes the number of galaxies in cell j , S_j is the value of the SF and $w_{ij} = W(\mathbf{r}_i - \mathbf{r}_j)$ a

smoothing kernel, which we here take to be a Gaussian of the form

$$W(\mathbf{x}) = \frac{1}{\pi^{3/2} \lambda^3} \exp\left(-\frac{|\mathbf{x}|^2}{\lambda^2}\right). \quad (31)$$

Then unbiased estimators for the mean \bar{d} and the variance σ^2 of the galaxy density field are given by

$$\bar{d} = \frac{\sum_i g_i d_i}{\sum_i g_i} \quad (32)$$

and

$$\sigma^2 = \frac{\sum_i h_i \left[\left(\frac{d_i - \bar{d}}{\lambda} \right)^2 - Y_i^{(2)} \right]}{\sum_i h_i}, \quad (33)$$

where

$$Y_i^{(n)} = \bar{d}^{1-n} \sum_j \frac{w_{ij}^n}{S_j^{n-1}}. \quad (34)$$

These estimators become minimum variance estimators in a good approximation if the weights are chosen as

$$g_i = \left[Y_i^{(2)} \right]^{-1} \quad (35)$$

and

$$h_i = \left[Y_i^{(4)} + 2 \left(Y_i^{(2)} \right)^2 + 2\sigma^4 + \left(3 \left(Y_i^{(2)} \right)^2 + 4Y_i^{(3)} + 4Y_i^{(2)} \right) \sigma^2 \right]^{-1}. \quad (36)$$

Since the estimate of the variance depends on the SF it becomes a function of the adopted evolutionary model used in computing the SF. It is therefore possible to estimate the evolutionary rate by minimizing σ^2 .

A difficulty with this technique is that it does not easily supply an error estimate for the evolutionary rate. Additionally it is unclear how to choose λ in an optimal way. A large λ allows the survey volume to be probed to greater depth, thereby increasing the sensitivity to evolution. However, the number of independent smoothing volumes declines simultaneously, thereby degrading the accuracy of the variance estimate. What is then the optimal choice?

We solve both of these problems by extracting an ensemble of mock catalogues from a large N-body simulation. The mock surveys mimic the statistical properties of the survey at hand in terms of the SF, the evolution, the sky coverage and the source density. This suite of catalogues can be used to find the optimal λ and to estimate the precision of the final evolutionary estimate.

Although computationally somewhat lengthy this scheme is well worth the effort because it offers an increased accuracy as we will demonstrate with the mock surveys in our application to the 1.2-Jy survey. A further advantage is that it is equally applicable to luminosity evolution, in contrast to the estimator discussed in section 4.2.

5 APPLICATION TO THE 1.2-JY REDSHIFT SURVEY

The data of the 1.2-Jy redshift survey (Strauss et al. 1990) of *IRAS* galaxies has been published (Fisher et al. 1995)

and can be retrieved electronically from the Astronomical Data Center (<ftp://adc.gsfc.nasa.gov>). The 5321 galaxies of the survey are selected from the PSC catalogue above a flux limit of 1.2 Jy in the 60 μm band. The sky coverage is 87.6 per cent, excluding only the zone of avoidance for $|b| < 5^\circ$ and a few unobserved or contaminated patches at higher latitude.

We convert the redshifts to the Local Group frame and use them subsequently to infer distances without further corrections for peculiar velocities.

5.1 K-correction and maximal redshift

The estimators presented above demand an accurate computation of the maximal redshift $z_i^{\text{m}} = z_{\text{max}}(L_i)$ that a given source could have without falling below the flux limit. A detailed calculation of this quantity involves K- and colour-corrections, which require a knowledge of the spectral energy distribution (SED) of the source, a specification of the responsivity $R(\nu)$ of the detector, and a choice for the cosmological background model.

For the case of the *IRAS* surveys Fisher et al. (1992) have phrased this problem in terms of the useful equation

$$\frac{f_{\text{min}}}{f_i} = \frac{r_i^2}{r(z_i^{\text{m}})^2} \frac{\Psi(\eta)}{\eta}, \quad (37)$$

which implicitly specifies z_i^{m} in a general form. Here f_i is the quoted flux density of a source and r_i is its comoving coordinate distance. f_{min} gives the flux limit of the catalogue and η is defined as $\eta = (1 + z_i^{\text{m}})(1 + z)^{-1}$. The function

$$\Psi(\eta) = \frac{\int R(\nu) f_\nu(\nu\eta) d\nu}{\int R(\nu') f_\nu(\nu') d\nu'} \quad (38)$$

encodes K- and colour-corrections by means of the observed flux density $f_\nu(\nu)$ of the source. The cosmological background model enters via the function $r = r(z)$. We will adopt an Einstein-de-Sitter universe, i.e.

$$r(z) = \frac{2}{a_0 H_0} \left(1 - \frac{1}{\sqrt{1+z}} \right). \quad (39)$$

The 60 μm band SED of *IRAS* galaxies might be approximated as a straight power law $L_\nu(\nu) \propto \nu^\alpha$ with $\alpha \approx -2$. In this case $\Psi(\eta) = \eta^\alpha$. We have typically used $\alpha = -2$, but also tried a gray-body model (Saunders et al. 1990) fitted to 60 $\mu\text{m}/100 \mu\text{m}$ flux ratios and the polynomial model of Fisher et al. (1992) which results in a considerably shallower SED.

5.2 Selection function

In our determination of the SF and LF we will assume that the LF exhibits density evolution of the form $g(z) = (1+z)^P$ with $P = 4.3$. The actual estimation of the evolutionary rate is discussed below in section 5.4.

Figure 1 shows the estimated local slopes m_k of the SF and a fit based on the functional form

$$S(z) = \frac{\psi}{z^\alpha \left(1 + \left(\frac{z}{z^*} \right)^\gamma \right)^{\beta/\gamma}}. \quad (40)$$

We used 40 redshift intervals, logarithmically spaced between $x_0 = 0.003$ and $x_{39} = 0.15$, for the non-parametric

Table 1. Parameters of the selection function fit.

α	β	γ
$0.741^{+0.128}_{-0.135}$	$4.210^{+0.419}_{-0.344}$	$1.582^{+0.237}_{-0.214}$
z^*	$\psi [h^3 \text{Mpc}^{-3}]$	
$0.0184^{+0.00213}_{-0.00167}$	$(486.5 \pm 13.0) \times 10^{-6}$	

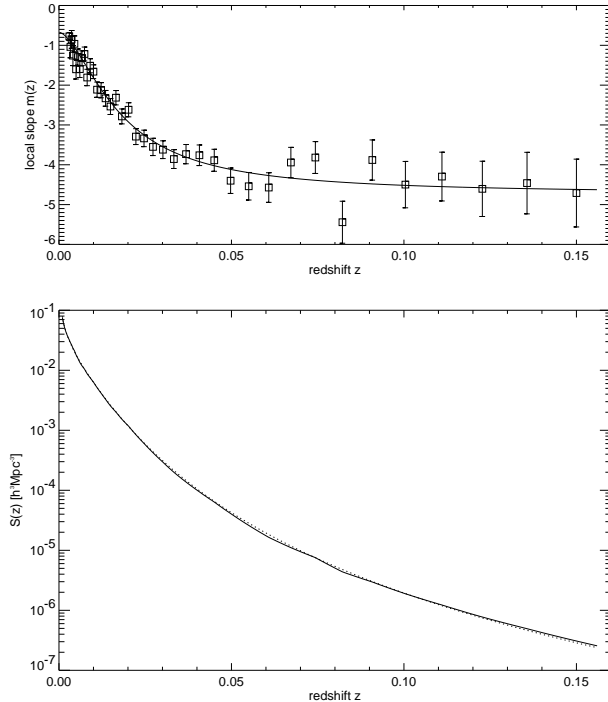


Figure 1. Non-parametric selection function estimate. The top panel shows the estimated slopes m_k with 1σ error bars. The fit is based on equation (40). The lower panel compares the actual non-parametric SF (solid) and the analytic fit (dotted) with the parameters of table 1.

estimate. A minimum χ^2 fit of the measured m_k to the form of equation (40) resulted in a reduced χ^2_ν of 0.87 (for $\nu = 36$ degrees of freedom), which indicates a good fit. This form of the SF is slightly more general than the one used by Yahil et al. (1991) and Fisher et al. (1995) who essentially fixed γ at the value 2. This gives a marginally worse χ^2_ν of 0.91.

Our best estimates for the final SF parameters are listed in table 5.2. They are obtained by maximizing the likelihood of the parametric form directly. Although a fit to the non-parametric estimate gives a very close result, we prefer these numbers as final estimates, because they are free of any binning effects. For each of the parameters α , β , γ , and z^* the quoted errors give 1σ confidence intervals obtained from the bounding box of the $\Lambda_{\text{max}} - 0.5$ likelihood contour.

Figure 2 shows the ratio of Fisher et al.'s (1995) SF to our estimate. The agreement is quite good out to redshift around 0.1. However, relative to our result the predicted mean density of galaxies at redshift 0.15 is about 20 per cent higher in the Fisher et al. (1995) result.

In order to normalize the SF we used the volume inside

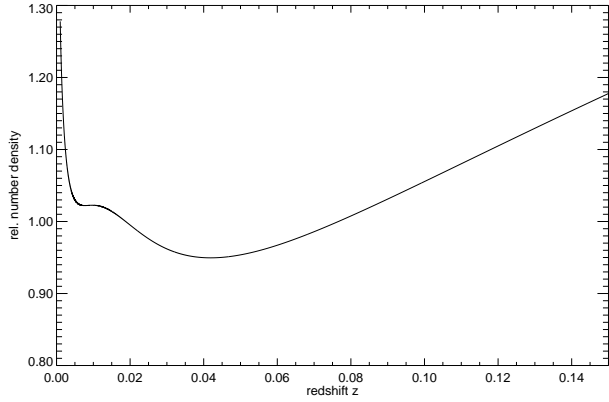


Figure 2. Ratio of the 1.2-Jy-SF of Fisher et al. (1995) to the result of this work. The ratio is scaled such that both parameterizations of the SF predict the same number of galaxies out to redshift 0.15.

$z = 0.15$. This determines the parameter ψ and results in $N = (490 \pm 13) \text{ sr}^{-1}$ expected galaxies per unit solid angle on the sky. Our final LF is also normalized to this number. The 1σ error-estimate is based on a direct computation of the variance of ψ by means of equation (19). Here the uncertainty in the shape of $s(z)$ is neglected.

5.3 Luminosity function

Figure 3 displays our non-parametric estimate of the far-infrared LF resulting from the method outlined in section 3. For comparison also shown is the non-parametric estimate of Saunders et al. (1990) which takes the form of a histogram because it uses step functions to model the LF. In order to facilitate a comparison with the literature we present the LF in terms of luminosity per decimal decade of luminosity, viz.

$$\phi(L) = \Phi_0(L) L \ln 10, \quad (41)$$

and we define L for a source with SED $L_\nu(\nu)$ as $L = \nu L_\nu(\nu)$ at $60 \mu\text{m}$.

We believe that our parameterization offers an improved description of the LF, without large unphysical jumps due to binning of sparse data. In particular, the quality of a fit with an analytic function can be judged quite easily.

As a fitting form we use the function

$$\phi(L) = C \left(\frac{L}{L_*} \right)^{1-\alpha} \left(1 + \frac{L}{L_*\beta} \right)^{-\beta} \quad (42)$$

proposed by Lawrence et al. (1986) and give the best-fit parameters in table 2. The fit is based on a minimization of the covariance form (25), imposing a fixed normalization as described in appendix A. The cited errors for α , β and L_* give 68.3 per cent confidence intervals derived from an increase of $\Delta\chi^2 = \chi^2 - \chi^2_{\text{min}}$ by 1, where $\Delta\chi^2$ is marginalized in the space of α , β , L_* , and C . Figure 4 shows contour levels of constant $\Delta\chi^2$ in the subspace of α and β . The contour of $\Delta\chi^2 = 2.3$ encloses the 68.3 per cent joint confidence region of α and β . The error given in table 2 for the normalization C is computed for a fixed shape of the LF.

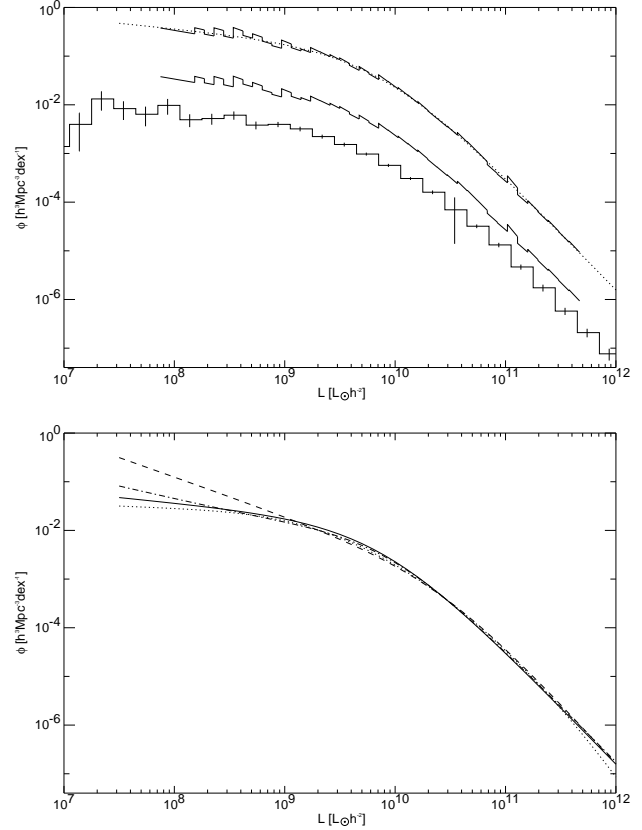


Figure 3. Luminosity function estimates. The top panel compares our non-parametric LF estimate (thick) with the estimate of Saunders et al. (1990). The latter has been rescaled to $H_0 = 100 h \text{ km s}^{-1}$ and shifted vertically for graphical clarity. The two upper curves (also shifted) compare the non-parametric estimate with our analytic fit.

The lower panel shows various analytic parameterization of the far-infrared LF by different authors: Saunders et al. (1990) (dotted), Yahil et al. (1991) (dot-dashed), Lawrence et al. (1986) (dashed), this work (thick).

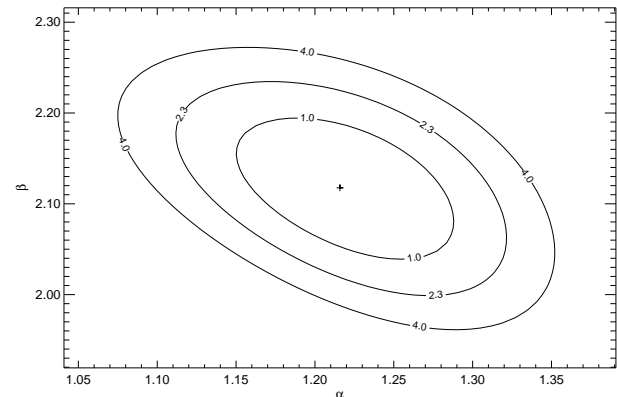


Figure 4. Contour levels of constant $\Delta\chi^2$ for the LF fit in the subspace of α and β . The thick contour defined by $\Delta\chi^2 = 2.3$ encloses the 68.3 per cent joint confidence region of α and β .

Table 2. Parameters of the luminosity function fit.

α	β
$1.221^{+0.068}_{-0.072}$	$2.116^{+0.080}_{-0.079}$
$L_{\star} [h^{-2}L_{\odot}]$	$C [h^3\text{Mpc}^{-3}]$
$3.615^{+0.640}_{-0.568} \times 10^9$	$(1.670 \pm 0.045) \times 10^{-2}$

The simple-two power law (42) does a remarkably good job in fitting the measurements as evidenced by the comparison in figure 3 and by a reduced χ^2_{ν} of 1.06. In particular we find no need to choose a functional form that shows more curvature over the full range of luminosities (Saunders et al. 1990). However, we must not forget that we have ignored velocity fields in this paper and that we cannot go as faint as Saunders et al. (1990) who used an additional set of very local galaxies. This might affect the faint end slope; we find a value not quite as shallow as Saunders et al. (1990), but somewhat flatter than Yahil et al. (1991).

5.4 Evolution

Evidence for evolution in *IRAS* galaxies has been reported by a number of authors using differential source counts (Hacking & Soifer 1991; Hacking, Condon & Houck 1987; Lonsdale et al. 1990; Gergorich et al. 1995) and redshift surveys (Lonsdale & Hacking 1989; Saunders et al. 1990; Fisher et al. 1992; Oliver et al. 1994). However, there has been some controversy about the magnitude of the evolutionary rate seen in the far-infrared LF. Saunders et al. (1990) found $P = 7 \pm 2$ for the QCD survey, whereas Fisher et al. (1992) gave $P = 2 \pm 3$ for the 1.2-Jy survey, a result apparently consistent with no evolution. Oliver et al. (1994) found $P = 6.25 \pm 1.5$ for a survey of faint *IRAS* galaxies and $P = 4.2 \pm 2.3$ for the QDOT survey. More recently Bertin et al. (1996) report $P = 6.0 \pm 1.2$ for the FIR sample.

The low result for the 1.2-Jy survey, obtained with the method of section 4.2, was based on an early version of the catalogue. Since evolutionary estimates are quite sensitive to completeness we here analyse the final catalogue again. This is also necessary because the evolutionary rate is needed as input parameter for the determination of the SF and LF.

5.4.1 The run of radial density

A first indication that a correct treatment of evolution is important may be obtained with the radial density estimator based on equation (27). We adopt a parameterization of $n_z(r)$ in terms of 45 step-functions (with $R_{\text{max}} = 400 h^{-1}\text{Mpc}$) of widths chosen such that the signal-to-noise ratio in each bin stays roughly constant.

In the resulting distribution, displayed in figure 5, the average density seems to rise with distance. A similar behaviour is also found if smaller patches of the sky are examined separately. As an illustration we have split the sample in 4 regions of approximately equal size selected in terms of the modulus $|b|$ of the galactic latitude. In this way we also obtain a low latitude sample which might be less complete than the other parts of the survey. In detail these regions, labeled B1-B4, cover $|b| < 18^\circ$ (B1), $18^\circ \leq |b| < 33^\circ$ (B2), $33^\circ \leq |b| < 52^\circ$ (B3), and $52^\circ \leq |b|$ (B4). As evidenced

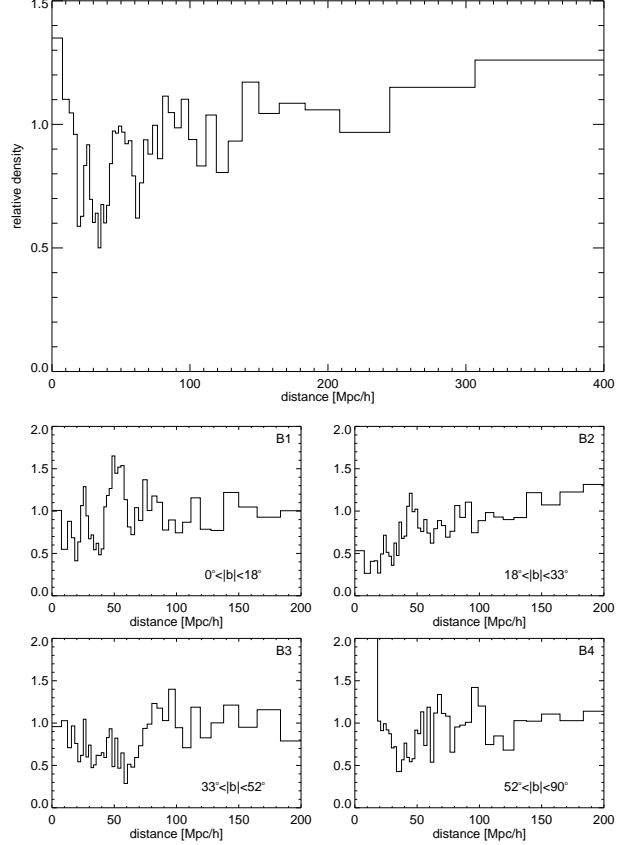


Figure 5. Radial density distribution obtained with a non-parametric estimator based on equation (27) and the assumption of no evolution. The result for the full sample is shown in the top panel, whereas the plots labeled B1–B4 are computed for subsamples selected by galactic latitude: $|b| < 18^\circ$ (B1), $18^\circ \leq |b| < 33^\circ$ (B2), $33^\circ \leq |b| < 52^\circ$ (B3), and $52^\circ \leq |b|$ (B4).

Table 3. Evolutionary estimates P obtained with the constant density method for various redshift intervals. The subsamples B1–B4 are selected in terms of galactic latitude: $|b| < 18^\circ$ (B1), $18^\circ \leq |b| < 33^\circ$ (B2), $33^\circ \leq |b| < 52^\circ$ (B3), and $52^\circ \leq |b|$ (B4).

	$[0, \infty]$	$[0.01, \infty]$	$[0, 0.1]$	$[0.01, 0.1]$
Full	3.7 ± 1.5	5.0 ± 1.6	3.9 ± 1.9	5.9 ± 2.0
B1	-1.0 ± 3.3	-1.5 ± 3.4	2.6 ± 3.9	2.5 ± 4.2
B2	9.2 ± 3.2	6.1 ± 3.2	11.1 ± 3.8	6.7 ± 3.9
B3	6.1 ± 3.1	7.8 ± 3.3	7.1 ± 3.7	9.7 ± 4.0
B4	0.6 ± 2.8	6.5 ± 3.1	-6.2 ± 3.8	4.1 ± 4.3

by figure 5 the rise of density with distance can be seen in all four subsamples, albeit with variable strength. Prominent structures are also visible, in particular Perseus-Pisces (around $50 h^{-1}\text{Mpc}$) and the Local Supercluster, which is responsible for the nearby overdensity seen in B4.

5.4.2 Evolutionary estimates with the constant density method

We now turn to estimates of the density evolution parameter P obtained with the estimator of section 4.2. Table 3 shows

results for various redshift intervals, in each case computed for the full catalogue and for the subsamples B1–B4.

Although the statistical errors are large, they are insufficient to explain the large differences in the estimates that result when the redshift boundaries are changed. For example, when the upper redshift cut-off is lowered from ∞ to 0.1, the low latitude sample B1 shows a marked increase in P which is likely to be the result of incompleteness at large z . The sample B4 on the other hand exhibits a very strong overdensity nearby, that biases evolution low if it is not excluded by imposing a lower redshift cut-off.

We have tried many different redshift intervals and find it hard to come to definite conclusions with this method, simply because the result is strongly affected by density inhomogeneities and the choice of a redshift interval exhibits a certain degree of arbitrariness. We therefore prefer to estimate evolution with the minimum variance method outlined in section 4.3.

5.4.3 An ensemble of mock surveys

In order to demonstrate that this method is indeed more reliable we have constructed an ensemble of 1.2-Jy-like mock catalogues by *observing* a large N-body simulation of a standard CDM universe. The simulation has been kindly provided by the Virgo collaboration (Jenkins et al. 1996). It contains 256^3 particles in a periodic box of size $V = L^3$ with $L = 240 h^{-1}\text{Mpc}$ and is normalized to fluctuations of $\sigma_8 = 0.6$ in spheres of $8 h^{-1}\text{Mpc}$. The details of this model are not of much relevance for the following, the salient point is that the model exhibits clustering in realistic strength.

By randomly placing an observer in the periodic box we constructed 50 mock catalogues of this simulation. We used a SF very similar to the 1.2-Jy survey (with parameters $\alpha = 0.84$, $\beta = 3.96$, $\gamma = 1.74$, $z^* = 0.018$) and imposed density evolution with $P = 5$. The mock catalogues featured the same angular mask as the 1.2-Jy survey and were sampled to a density of 5321 galaxies inside $460 h^{-1}\text{Mpc}$. The suite of these catalogues simulates Poisson sampling noise and – to a reasonable degree – cosmic variance as well. The catalogues can be ideally used to test the performance of the various estimators discussed in this paper.

First we applied the constant density estimator of section 4.2 to these catalogues. Using the redshift interval $[0, 0.1]$ we obtained $\langle P \rangle = 5.7$ with an rms scatter of 2.4 among the individual measurements. This scatter is somewhat larger than the statistical error of ≈ 1.9 provided by the likelihood method itself. Smaller redshift intervals also led to estimates $\langle P \rangle$ close to 5, however with larger scatter.

Next we applied our new minimum variance method to the mock catalogues. For this purpose we computed maximum likelihood SF fits for 11 different values of P in the range 0 to 10 individually for each catalogue. This allows the computation of a curve $\sigma_\lambda^2(P)$ for each catalogue, and – by fitting the minimum with a parabola – an estimate of P .

We treated the technical difficulty of the presence of an angular mask in the surveys by using the ratio method of Melott & Dominik (1993) in the smoothing process. This means that we actually chose

$$w_{ij} = \frac{W(\mathbf{r}_i - \mathbf{r}_j)}{\int W(\mathbf{r}_i - \mathbf{r}')M(\mathbf{r}')d\mathbf{r}'} \quad (43)$$

as kernel in equation (30), where $M(\mathbf{r})$ is a field equal to 1 in the actual survey volume and equal to 0 in the volume behind the angular mask. The estimation of the variance is only done with cells inside the survey volume.

The method finally requires the choice of a smoothing length λ . Since the minimum variance estimator automatically turns off when the signal-to-noise ratio becomes too low a larger λ usually means that the survey is probed to higher depth, thereby increasing the sensitivity to evolution. On the other hand, the accuracy of the measurement of the variance degrades with increasing λ because the number of independent smoothing volumes in the usable survey volume declines. We find a choice for λ that represents a compromise between these two effects by minimizing the rms scatter of the P measurements for the mock catalogues.

For this purpose we have computed estimates of $\langle P \rangle$ and its scatter for a range of smoothing lengths and find that the uncertainty is smallest for $\lambda \simeq 60 h^{-1}\text{Mpc}$, however, any λ in the range $50\text{--}80 h^{-1}\text{Mpc}$ works almost equally well. For $\lambda = 60 h^{-1}\text{Mpc}$ we obtain $\langle P \rangle = 5.3$ with rms fluctuations of 1.4. This is a considerable improvement compared to the constant density method, nearly cutting the random error in half. This is possible because the new method eliminates most of the systematic influence of density inhomogeneities on the estimate of P . The remaining uncertainty is mainly due to counting statistics.

5.4.4 Evolutionary estimate with the minimum variance method

The above results show that the new estimator for density evolution gives a more precise estimate than the constant density method. Hence we apply it now to obtain our best estimate for the density evolutionary rate of the 1.2-Jy survey. Adopting $\lambda = 60 h^{-1}\text{Mpc}$ and using the same procedure as applied to the mock surveys we find $P = 4.31 \pm 1.4$, where the error estimate is based on the mock surveys.

Clearly, this error estimate is somewhat too optimistic, because the 1.2-Jy survey is not as perfectly selected as the mock catalogues. Additionally there are a number of systematic uncertainties that degrade the accuracy of the evolutionary measurement.

For example, the SED might be shallower as we assumed here, leading to an overestimate of evolution. The gray-body model (we find $P = 3.9$) does only very little change compared to the straight $\alpha = -2$ SED used here. On the other hand, Fisher et al.’s (1992) significantly flatter polynomial model lowers the evolutionary rate quite strongly to $P = 3.0$. However, the SED of this model is likely to be too flat. In addition to $60 \mu\text{m}$ and $100 \mu\text{m}$ it tries to simultaneously fit the $25 \mu\text{m}$ fluxes which are typically underpredicted by the gray-body model. However, only half of the galaxies (the bright ones at $25 \mu\text{m}$) have detections in this band at all, so the polynomial model is biased towards a shallow SED. The polynomial model will also underpredict the slope of the SED if the spectra are indeed comprised of a cool and a warm component, as seems often to be the case (Rowan-Robinson & Crawford 1989).

Because the 1.2-Jy survey is quite local, a change of background cosmology to a low density universe has very little effect, increasing the estimated P very slightly.

More serious are potential problems with the *IRAS*

flux scale. Either a baseline flux error with accompanying Malmquist bias, or a nonlinear flux scale could lead to a significant overestimate of the evolutionary rate. However, so far there is no convincing evidence that the *IRAS* PSC is troubled with flux errors of the strength required to explain a significant fraction of the evolutionary signal. For example, Oliver et al. (1994) give an upper limit of 36 mJy for the baseline flux error of the PSC. At this level, Malmquist bias is not an issue, as we have checked with mock surveys that exhibit artificial flux errors.

We believe that our new method for estimating the evolutionary rate has removed most of the uncertainty due to density inhomogeneities. However, sample incompleteness can bias the evolution low if a fraction of the faint high redshift objects is missed. At low latitude, this is indeed quite likely the case for the 1.2-Jy survey.

We think that an error of ± 1 represents a reasonable estimate of these systematic uncertainties. Our final estimate for evolution is therefore $P = 4.3 \pm 1.4 \pm 1$. Given the uncertainties, this result is in good agreement with other determinations of P cited above. However, it is notably higher than Fisher et al.'s (1992) result for an early version of the 1.2-Jy survey.

6 DISCUSSION

An accurate determination of the SF of a redshift survey is a prerequisite for taking full advantage of its information about the large-scale structure of the Universe. For example, statistical methods that rely on estimates of the density field in large survey volumes, like power spectrum measurements or genus statistics, depend crucially on a precise knowledge of the mean density as a function of distance.

In this work we have proposed a flexible non-parametric maximum likelihood estimator for the SF and LF. The method is independent of density inhomogeneities, gives accurate information on the shapes of SF and LF, and provides estimates of the statistical uncertainties of the derived quantities with relative computational ease. We think that the technique should be useful for upcoming redshift surveys.

We have also proposed a new method to estimate evolution of the LF, based on the notion that the Universe should look homogeneous on large scales. With an ensemble of mock surveys we have demonstrated that the uncertainties due to density inhomogeneities, which troubled previous estimators, can be greatly reduced in this way.

In our application of these estimators to the 1.2-Jy survey of *IRAS* galaxies we have found evidence for strong evolution, confirming reports by several previous authors. Expressed in terms of density evolution $\propto (1+z)^P$, we find $P = 4.3 \pm 1.4 \pm 1$. This high evolutionary rate for the far-infrared LF is hard to explain as a statistical fluke. If confirmed the strong evolution of the far-infrared LF will represent an interesting challenge for theories of galaxy formation, interaction and evolution.

REFERENCES

- Avni Y., Bahcall J. N., 1980, ApJ, 235, 694
 Bertin E., Dennefeld M., Moshir M., 1996, astro-ph/9610218
 Davis M., Huchra J., 1982, ApJ, 254, 437

- Efstathiou G., Ellis R. S., Peterson B. A., 1988, MNRAS, 232, 431
 Fisher K. B., Strauss M. A., Davis M., Yahil A., Huchra J. P., 1992, ApJ, 389, 188
 Fisher K. B., Huchra J. P., Strauss M. A., Davis M., Yahil A., Schlegel D., 1995, ApJS, 100, 69
 Gregorich D. T., Neugebauer G., Soifer B. T., Gunn J. E., Herter T. L., 1995, AJ, 110, 259
 Hacking P. B., Soifer B. T., 1991, ApJ, 367, L49
 Hacking P., Condon J. J., Houck J. R., 1987, ApJ, 316, L15
 Jenkins A., Frenk C. S., Pearce F. R., Thomas P. A., Hutchings R., Colberg J. M., White S. D. M., Couchman H. M. P., Peacock J. A., Efstathiou G. P., Nelson A. H., 1996, astro-ph/9610206
 Kendall M. G., Stuart A., 1979, The advanced theory of statistics. Charles Griffin, London, vol. 2
 Lawrence A., Walker D., Rowan-Robinson M., Leech K. J., Penston M. V., 1986, MNRAS, 219, 687
 Lin H., Kirshner R. P., Shectman S. A., Landy S. D., Oemler A., Tucker D. L., Schechter P. L., 1996, ApJ, 464, 60
 Lonsdale C. J., Hacking P. B., 1989, ApJ, 339, 712
 Lonsdale C. J., Hacking P. B., Conrow T. P., Rowan-Robinson M., 1990, ApJ, 358, 60
 Loveday J., Peterson B. A., Efstathiou G., Maddox, S. J., 1992, ApJ, 390, 338
 Melott A. L., Dominik K. G., 1993, ApJS, 86, 1
 Nicoll J. F., Segal I. E., 1983, A&A, 118, 180
 Oliver S. J., Rowan-Robinson M., Saunders W., 1992, MNRAS, 256, 15P
 Oliver S., Broadhurst T., Rowan-Robinson M., Saunders W., Lawrence A., McMahon R., Lonsdale C., Hacking P., Taylor A., Conrow T., 1994, in Maddox S. J., Aragón-Salamanca A., eds, 35th Herstmonceux Conference, Wide Field Spectroscopy and the Distant Universe. World Scientific, Singapore, p. 274
 Rowan-Robinson M., Crawford J., 1989, MNRAS, 238, 523
 Sandage A., Tammann G. A., Yahil A., 1979, ApJ, 232, 352
 Saunders W., Rowan-Robinson M., Lawrence A., Efstathiou G., Kaiser N., Ellis R. S., Frenk C. S., 1990, MNRAS, 242, 318
 Saunders W., Frenk C., Rowan-Robinson M., Efstathiou G., Lawrence A., Kaiser N., Ellis R., Crawford J., Xiao-Yang X., Parry I., 1991, Nature, 349, 32
 Schmidt M., 1968, ApJ, 151, 393
 Strauss M. A., Davis M., Yahil M., Huchra J. P., 1990, ApJ, 361, 49
 Turner E. L., 1979, ApJ, 231, 645
 Yahil A., Strauss M. A., Davis M., Huchra J. P., 1991, ApJ, 372, 380

APPENDIX A: COVARIANCE MATRIX OF THE NON-PARAMETRIC LUMINOSITY FUNCTION ESTIMATE

In this section we compute the covariance matrix

$$V_{kl} = \text{cov}(\ln \Phi_k, \ln \Phi_l) \quad (\text{A1})$$

of the non-parametric LF estimate. Because we are primarily interested in the uncertainty of the shape of the LF we impose a fixed normalization, i.e. the quantity

$$N' = \int_0^{x_n} S(z) z^2 dz = S_1 Q \quad (\text{A2})$$

is held constant. Here $Q = Q(m_1, \dots, m_n)$ is given by

$$Q = \sum_{k=1}^n \frac{x_k^3}{m_k + 3} \left[1 - \left(\frac{x_{k-1}}{x_k} \right)^{m_k + 3} \right] \prod_{j=2}^k \left(\frac{x_j}{x_{j-1}} \right)^{m_j}. \quad (\text{A3})$$

Then $\ln \Phi_k$ may be expressed as

$$\begin{aligned} \ln \Phi_k &= \ln \left(\frac{g'(x_k)}{g(x_k)} - \frac{m_k}{x_k} \right) + \sum_{j=2}^k m_j \ln \frac{x_j}{x_{j-1}} \\ &\quad - \ln Q + \ln \frac{N'}{g(x_k)L'_{\min}(x_k)}. \end{aligned} \quad (\text{A4})$$

An expansion of $\ln \Phi_k$ to linear order in the slopes m_i allows an estimate of the covariance matrix in the form

$$V_{kl} = \sum_{i=1}^n A_{ki} A_{li} \text{var}(m_i), \quad (\text{A5})$$

where we have defined

$$A_{ki} = \frac{\partial \ln \Phi_k}{\partial m_i}. \quad (\text{A6})$$

The expressions for A_{ki} are somewhat lengthy, yet straightforward to calculate:

$$\begin{aligned} A_{ki} &= \frac{\delta_{ki}}{m_k - x_k \frac{g'(x_k)}{g(x_k)}} + \sum_{j=2}^k \delta_{ij} \ln \frac{x_i}{x_{i-1}} \\ &\quad - \frac{1}{Q} \left\{ U_i - \frac{S_i}{S_1} \frac{x_i^3}{(m_i + 3)^2} \right. \\ &\quad \left. \times \left[1 - \left(\frac{x_{i-1}}{x_i} \right)^{m_i+3} \left(1 - (m_i + 3) \ln \frac{x_{i-1}}{x_i} \right) \right] \right\}. \end{aligned} \quad (\text{A7})$$

Here U_i is given by

$$U_i = \ln \frac{x_i}{x_{i-1}} \sum_{l=i}^n \frac{S_l}{S_1} \frac{x_l^3}{m_l + 3} \left[1 - \left(\frac{x_{l-1}}{x_l} \right)^{m_l+3} \right] \quad (\text{A8})$$

for $i > 1$ and by $U_i = 0$ for $i = 1$.